

Dual Coordination between Stereochemistry and Cations Endows Polyethylene Terephthalate Fabrics with Diversiform Antimicrobial Abilities for Attack and Defense

Pengfei Zhang, Xinyu Chen, Fanqiang Bu, Chen Chen, Lifei Huang, Zixu Xie, Guofeng Li, and Xing Wang*



Cite This: <https://doi.org/10.1021/acsami.2c19323>



Read Online

ACCESS |



Metrics & More



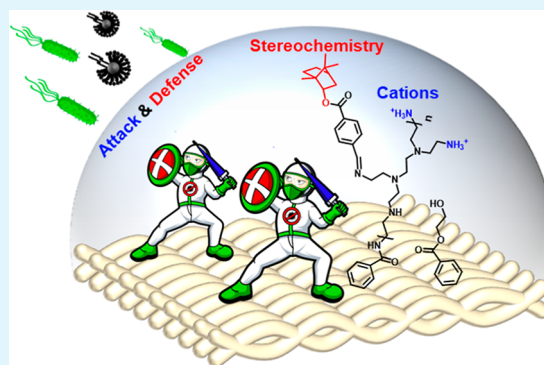
Article Recommendations



Supporting Information

ABSTRACT: Modification of fabrics by stereochemical antiadhesion strategies is an emerging approach to antimicrobial fabric finishing. However, a purely antiadhesive fabric cannot avoid the passive adhesion of pathogenic microorganisms. To address this issue, borneol 4-formylbenzoate (BF) with a stereochemical structure is introduced into a cationic polymer PEI-modified PET fabric by a simple two-step method. The obtained fabric exhibits remarkable features of high bactericidal activity, excellent resistance to bacterial adhesion, desirable fungal repellent performance, and low cytotoxicity. More impressively, this modified fabric not only effectively reduces microbial contamination during food preservation but also plays a role in avoiding infection and accelerating wound healing in the mouse wound model. The dual coordination between stereochemistry and cations is validated as a viable “attack and defense” antimicrobial strategy, providing an effective guide for diversiform antimicrobial designs.

KEYWORDS: PET fabric, PEI, stereochemistry, bactericidal activity, antifungal adhesion



1. INTRODUCTION

Polyethylene terephthalate (PET) fabrics have been used in a wide range of applications such as apparel, food packaging, and medical materials due to their excellent mechanical strength, ease of processing, quick drying, and dimensional stability.^{1,2} However, PET fabrics are usually porous three-dimensional structures that are vulnerable to the growth of host microorganisms and serve as a transfer medium for pathogens causing potential microbial cross-contamination.^{3–5} In addition, fungal contamination of PET fabrics under humid environments is also very serious, which can easily cause irreversible cosmetic damage to the fabrics.⁶ Therefore, it is of great importance to endow PET fabrics with diversiform antimicrobial abilities.

A series of antimicrobial finishing processes have been developed to solve these problems, the most common of which are spraying and grafting processes. Known for its simplicity and speed, the spraying process is usually achieved by spraying antimicrobial substances such as cationic polymers,⁷ nanoparticles,⁸ and plant essential oils⁹ directly onto PET fabrics. Compared with the spraying method, the surface grafting finishing method is more tedious, but the finished PET fabrics generally exhibit better antimicrobial durability. In order to realize the grafting and finishing of PET, the first step is to activate PET.^{10,11} Various activation methods have been

developed, such as alkaline hydrolysis,¹² ammonolysis,¹³ plasma treatment,¹⁴ γ -ray radiation,¹⁵ or UV radiation¹⁶ to introduce reactive groups. Among them, the functionalization of inert PET with polyethyleneimine (PEI) by ammonolysis has attracted a lot of attention from researchers.¹⁷ On the one hand, the modification of PEI can provide amino active sites for subsequent modifications. On the other hand, as a typical cationic polymer, PEI endows the fabrics with good bactericidal activity. However, the cytotoxicity of fabrics due to PEI is a critical issue that cannot be ignored.¹⁸

Recently, stereochemical antiadhesion strategies have attracted widespread interest, of which borneol with stereochemical structures is a representative monomer.^{19–23} It has been reported that the synergistic effect of borneol and quaternary ammonium salts,²⁴ fluoropolymers,²⁵ zwitterions,²⁶ and sugar-containing polymers²⁷ can impart excellent antibacterial and antifouling properties to the materials. However, since these coatings are not bactericidal, some passive adhesion

Received: October 27, 2022

Accepted: January 23, 2023

of pathogenic bacteria is inevitable. Zhang et al. proposed a “repel-kill” strategy, which provides a new idea to solve this problem.²⁸ Therefore, in order to achieve a better antimicrobial effect of borneol-modified material, an antiadhesive surface should be provided along with a bactericidal surface to rapidly kill pathogenic microorganisms on contact and invasion, thus achieving an “integrated offensive and defensive” strategy against pathogenic microorganisms.

Herein, we propose a rapid and economical finishing approach based on dual coordination between stereochemistry and cations. An antimicrobial PET fabric is prepared using the cationic polymer (PEI) with the stereochemical unit (borneol) as an antimicrobial finishing agent via the aminolysis and Schiff base reactions. The stereochemical structure of borneol constructs the antiadhesive layer, which realizes the first defense against microorganisms. The cationic polymer PEI builds the bactericidal layer and achieves the second defense against microorganisms. The combination of these two forms an “integrated offensive and defensive” antimicrobial system, thus compensating for the shortcomings of each. To our knowledge, no similar combination of a cationic bactericidal strategy and a stereochemical antiadhesion strategy for antimicrobial polyesters has been reported. The obtained antimicrobial textiles have promising applications in healthcare and packaging. It is noteworthy that the combination of both strategies can also be extended to the antimicrobial modification of other materials.

2. MATERIALS AND METHODS

2.1. Materials. A 100% PET fabric (200 g/m²) was provided by Dongguan Huamei Co (Guangdong China). PEI with different molecular weights ($M_w = 600, 1800, \text{ and } 10000 \text{ Da}$, >99%), malt extract agar, tryptone soy agar (TSA), and trypticase soy broth (TSB) were purchased from Aladdin Ltd (Shanghai, China). Borneol 4-formylbenzoate (BF) was synthesized according to the method previously reported by our group.²⁹ All reagents were analytically pure and were supplied by Damao Chemical Factory (Tianjin, China). *E. coli* (ATCC 25922), *S. aureus* (ATCC 25923), *M. racemosus* (CICC 3161), and *A. niger* (CICC 41254) were obtained from the China Center of Industrial Culture Collection. BALB/c male mice (5–6 weeks) were purchased from Beijing Charles River Co., Ltd. All animals were treated and cared for in accordance with the National Research Council's Guide for the care and use of laboratory animals and under the supervision and assessment by the SPF Animal Department of Clinical Institute in China-Japan Friendship Hospital (Approval no. Zryhy 12-20-08–3).

2.2. Aminolysis Reactions of PET. The PET fabric was washed in dichloromethane (DCM), acetone, and methanol solutions for 20 min using an ultrasonic cleaner to remove residual commercial additives and dried overnight at 60 °C under vacuum. A piece of the PET fabric (5 cm × 5 cm) was immersed in the 10 wt % PEI/methanol mixture with continuous stirring at 50 °C for 4 h. The PET fabric was then washed with an excess of methanol solution to remove residual PEI and dried under vacuum overnight. PET modified with different PEI molecular weights was named PET-1 ($M_w = 600 \text{ Da}$), PET-2 ($M_w = 1800 \text{ Da}$), and PET-3 ($M_w = 10000 \text{ Da}$).

2.3. Grafting BF via the Schiff Base. The graft of BF was synthesized via the Schiff base reaction between amino groups from PEI and aldehyde groups from BF. PET-1, PET-2, and PET-3 were immersed in a BF/methanol solution (0.01 g/mL), and the reaction mixture was stirred at room temperature for 8 h. The fabric was then washed with methanol to remove residual BF and dried under vacuum for at least 12 h. The fabrics obtained were named PET-1', PET-2', and PET-3'.

2.4. Characterization. A scanning electron microscope (JSM-7800 FJEOL, Tokyo, Japan) was used to observe the surface

morphology of the fabrics at an acceleration voltage of 10 kV. Attenuated total reflectance Fourier transform infrared (ATR-FTIR, Perkin-Elmer Spectrum 100 Spectrometer, Waltham, MA, USA) spectroscopy was used to analyze the surface chemical structure of the fabrics. X-ray photoelectron spectroscopy (XPS, Thermo Fisher Scientific, Waltham, MA, USA) was used to analyze the changes in surface elements before and after sample modification. The goniometer Kino SL200B was applied to measure static water contact angles (WCAs) (10 μL) to assess fabric surface wettability.

2.5. Quantification of Amino Groups in the Fabric. According to the previous report, the quantification of amino groups in fabric was measured by the orange II method.¹⁷ The fabric was immersed in an acidic environmental dye solution (6 mL, 40 mmol/L, pH = 6) for 20 min at 40 °C. The fabric was then washed intensively with the acidic solution (pH = 6) until there was no release of color. After air drying, the colored film was immersed in 6 mL of alkaline solution (pH = 12), and the dye was desorbed. The desorbed dye solution was adjusted to pH = 6 with a dilute HCl solution. The absorbance of the obtained solution was measured at 484 nm using a UV–vis spectrometer (UV765, Shanghai Manning Precision Science Co., Ltd). The concentration of the amine was determined from the corresponding calibration curve

$$y = 7.9488x + 0.0054, R^2 = 0.9996 \quad (1)$$

2.6. Antibacterial Assay. **2.6.1. Preparation of Bacterial Suspensions.** The bacterial strains (*E. coli* and *S. aureus*) were incubated in a fresh TSB medium overnight at 37 °C and then harvested by centrifugation at 6000 rpm for 5 min. Bacterial cells were washed five times with 2 mL of sterile saline to remove soluble nutrients. The resulting bacterial suspension was diluted to a concentration of 10⁷ CFU/mL with saline for later use.

2.6.2. Bactericidal Activity Assay. The bactericidal activity of fabrics against bacteria (*E. coli* and *S. aureus*) was evaluated according to the standard protocol of AATCC 100 with slight modifications.³⁰ The bacterial suspension (30 μL, 10⁷ CFU/mL) was added and sandwiched between two pieces of sterilized fabric samples (1 cm × 1 cm). Sandwich structures were incubated at 37 °C for 24 h, and a moist environment was maintained throughout the incubation to prevent fabrics from drying out. The fabric was then transferred to a centrifuge tube, and 2 mL of sterile saline was added. The sample was washed with sterile saline under vigorous agitation to effectively wash the bacterial cells from the fabric surface. Serial dilutions of 0.1 mL of the eluate were performed with 10-fold dilution and then coated on TSA plates. These plates were incubated at 37 °C for 12 h, and the number of cfus was manually counted to determine the antimicrobial effect of the fabrics. Each fabric sample was tested in triplicate. The antimicrobial performance of the modified fabric compared to the original fabric was calculated in terms of bacterial survival (%)

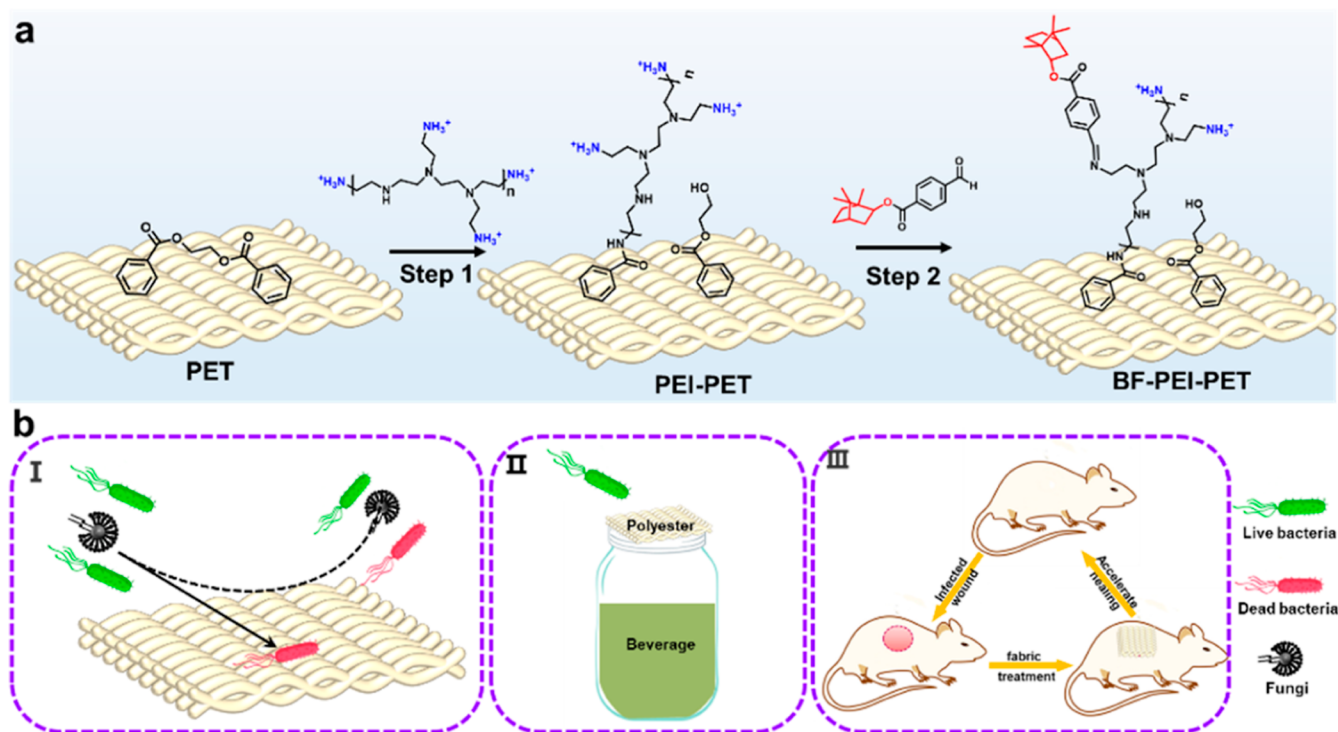
$$\text{antimicrobial efficiency (\%)} = (A - B)/A \times 100 \quad (2)$$

where *A* and *B* are the colony-forming units (CFUs) of raw PET and modified PET, respectively.

2.6.3. Bacterial Adhesion Assay. The resistance of fabrics to bacterial (*E. coli* and *S. aureus*) adhesion was evaluated according to the modified GB/T 20944.3–2008 method and ASTM E2149 method.³¹ In brief, the UV-sterilized fabrics were incubated in 3 mL of the bacterial suspension (10⁷ CFU/mL) in a shaker at 37 °C for 24 h. Then, after three gentle rinses with sterile saline, the bacteria firmly adhering to the sample surface were dispersed into 3 mL of sterile saline by vigorous stirring. Finally, 0.1 mL of the dispersion was taken out and serially diluted with sterile saline. The diluted bacterial solution (0.1 mL) was evenly coated on the TSA medium and incubated at 37 °C for 24 h. The number of cfus was calculated manually, and the number of adherent bacteria was calculated by multiplying the number of colonies by the dilution factor. Each fabric sample was tested in triplicate. The bacterial adhesion performance of the modified fabric compared to the original fabric was calculated in terms of the number of colonies (%)

$$\text{antiadhesion efficiency (\%)} = (A - B)/A \times 100 \quad (3)$$

Scheme 1. (a) Preparation of PET Fabrics with Diversiform Antimicrobial Abilities by Two-Step Finishing; (b) Application of the Modified Fabrics (I): Antibacterial and Antifungal; (II): Food Preservation; and (III): Infected Wound Treatment



where *A* and *B* are the colony-forming units (CFUs) of raw PET and modified PET, respectively.

2.6.4. SEM Images. For SEM imaging, the fabrics were gently rinsed three times with sterile saline and then completely immersed in a 2.5 wt % glutaraldehyde solution and placed at 4 °C for 2 h to fix the bacteria. The fabrics were then dehydrated in the gradients of 10, 30, 50, 70, 90, and 100 wt % ethanol/water solutions. After drying and sputter coating with Au, the fabrics were observed by SEM.

2.6.5. Zone of Inhibition Assay. The zone of inhibition (ZOI) experiment was used to test whether the fabric killed the bacteria by releasing small molecules. In brief, the bacterial suspension (0.1 mL, 10^7 CFU/mL) was added dropwise on the TSA medium, and then the bacterial suspension was spread evenly with a spreader. The fabric was then placed in the center of the medium and incubated at 37 °C for 24 h. The experimental phenomena were recorded using a digital camera.

2.7. Antifungal Assay. **2.7.1. Preparation of Fungal Suspensions.** The fungi (*A. niger* and *M. racemosus*) were incubated separately on a malt extract agar medium at 30 °C for 7 d using the plate scribing method. The fungal spores were then eluted with 5 mL of 0.9 wt % saline, collected, and uniformly dispersed. For the antifungal experiment, the concentration of the spore suspension was adjusted to approximately 10^8 CFU/mL.

2.7.2. Fungal Repelling Assay. *A. niger* and *M. racemosus* were chosen as typical fungal strains to assess the ability of the fabric to resist fungal adhesion according to the previously reported method.^{32,33} First, 2 μ L of the fungal suspension was added to the center of the plate. Next, the circular fabric (diameter = 15 mm) was placed approximately 15 mm from the center. Incubation was carried out in a mold incubator at 30 °C. The growth phenomena of the fungi were observed and recorded using a camera at different times.

2.7.3. Fungal Killing Assay. A simple contact killing method was used to investigate whether the fabric had a fungicidal effect. The *A. niger* suspension (30 μ L, 10^8 CFU/mL) was added and sandwiched between two pieces of sterilized PET-3' (1 cm \times 1 cm). Sandwich structures were incubated at 30 °C for 24 h, and a moist environment was maintained throughout the incubation to prevent fabrics from drying out. Subsequently, the PET-3' fabric was inverted in the

medium by the "stamp" method, and the fabric was removed after 30 s (the position where the fabric was placed is marked). The medium was incubated in an incubator at 30 °C for 7 d to observe the growth of *A. niger*. In addition, the microscopic morphology of *A. niger* (after 24 h of contact with PET-3')

2.8. Cytotoxicity Assays. **2.8.1. Cytotoxicity Test.** Mouse fibroblast (L929) cells were selected for the cytotoxicity assessment of PET, PET-3, and PET-3' by the MTT method.^{32,34} Cell suspensions that had successfully undergone recovery and passaging were added to 96-well plates, and then the 96-well plates were placed in an incubator for 24 h. Sterilized PET, PET-3, and PET-3' fabrics (0.05 g) were added to the culture plates, and 10% FBS, 100 units/mL penicillin, and 100 μ g/mL streptomycin were added to each well of the culture plates. The plates were then placed in an incubator for incubation at 48 h, and cell viability was determined using the MTT kit.

2.8.2. Fluorescent Images. The live/dead cell viability assay was used to observe the viability of cells after treatment with fabric samples. In brief, cells and fabrics were coincubated for 48 h and washed twice with PBS. Under light-proof conditions, 50 μ L of the live/dead staining solution was added to each well and protected from light for 15 min. Next, the cells were carefully rinsed twice with PBS to wash away the unbound dye. Finally, fluorescent images were taken under a fluorescent microscope.

2.9. Potential for Practical Applications. **2.9.1. Application of Food Preservation.** To explore the potential of antimicrobial PET fabrics for food preservation, a simple experiment was designed in which both water and milk were selected as the study subjects. In brief, PET-3' was sterilized with a 75% aqueous ethanol solution and air-dried on an ultraclean bench for 24 h. Then, 18 mL of beverages (water or milk) were placed in sterilized glass bottles. The fabric was tied around the mouth of the glass bottle, and the bottles were placed in an indoor environment. An aliquot of the beverage (100 μ L) was removed at the indicated time point and evenly applied to the surface of the TSA plate. These plates were incubated at 37 °C before observation. The PET fabric and special bacterial filter film were used as comparative tests. The percentage of area occupied by bacteria in the plates was quantified using Image J software.

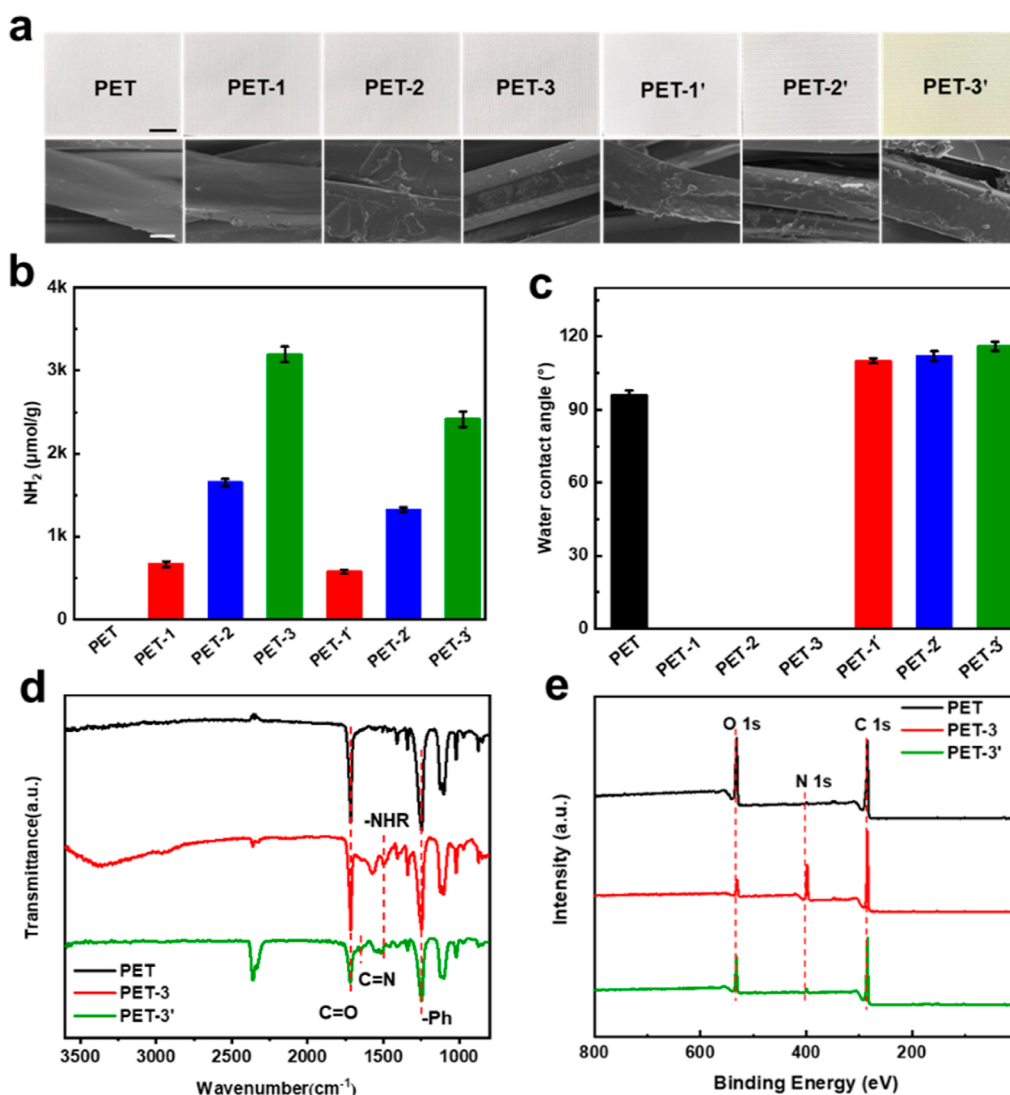


Figure 1. Characterization of PET and modified PET. (a) Digital photos and micromorphology. The scale bar in the image is 1 cm (black) and 10 μm (white). (b) Quantification of surface amino groups. (c) WCA. (d) ATR-FTIR spectra. (e) XPS spectra.

2.9.2. Application of Wound Dressing. The establishment of the mouse injury model was based on the previous literature to assess the wound healing of bacterial infections in modified fabrics.^{35,36} Before the test, the fabrics were sterilized in 75 wt % ethanol and irradiated with ultraviolet light for 1 h. In this study, male BALB/c mice aged 6–8 weeks (weighing 12–16 g) were used as study subjects and allowed to acclimatize for 7 d in the laboratory. The mice were randomly divided into three groups with three mice in each group ($n = 3$) according to the different treatments. The PET-3' group was selected as the experimental group, and the no treatment-only infection group and the PET group were selected as the control group. Before surgery, all mice were anesthetized intraperitoneally with sodium pentobarbital. Subsequently, a 10 mm diameter wound on the back of the mouse was created using a scalpel and a pressure mold ($d = 10$ mm). Then, the *S. aureus* suspension (20 μL , 1×10^8 CFU/mL) was dispersed uniformly into the wound to cause infection. A 15 mm diameter fabric was applied to the infected wound and secured with tape to prevent detachment. The wound healing process was photographed using a camera at different time intervals (0, 3, 7, 10, and 14 days). Wound healing was assessed from the percentage of wound healing rate. The wound area was measured using Image J software and the following formula³⁷

$$\text{WC} = (S_0 - S_t) / S_0 \times 100\% \quad (4)$$

where S_0 is the initial area of the created wound and S_t is the wound area at time t . WC is the wound healing rate.

2.10. Mechanical Performance. The tensile strength and elongation at the break of textiles (warp and cotton yarns) were evaluated according to GB/T 3923.1–1997 standards. Each sample was tested five times, and the average value was calculated.

2.11. Washing Durability Assays. To study the washing durability of the fabric, the standard method FZ/T 73023–2006 was used to evaluate the antimicrobial ability of PET-3' after 50 washes, according to previous reports.²¹ Each cycle was performed in a household washing machine with a regular detergent and 40 °C water (2 g/L). In a typical wash cycle, fabrics were washed for 2 min and spun for 30 s, recorded as one cycle. The fabrics' fungal repelling and bactericidal activities were evaluated after 50 consecutive washing cycles. To avoid the effects of residual detergents, fabrics should be washed with plenty of water and dried in the air before conducting antimicrobial tests. In addition, the changes in the WCA and surface chemical structure were evaluated before and after washing.

2.12. Statistical Analysis. Statistical analysis was performed with SPSS 16.0 software. All quantitative data were expressed as mean \pm standard deviation. After confirmation of normal distribution, two-tailed Student's t -tests were performed to assess differences between groups; p -values < 0.05 were considered statistically significant.

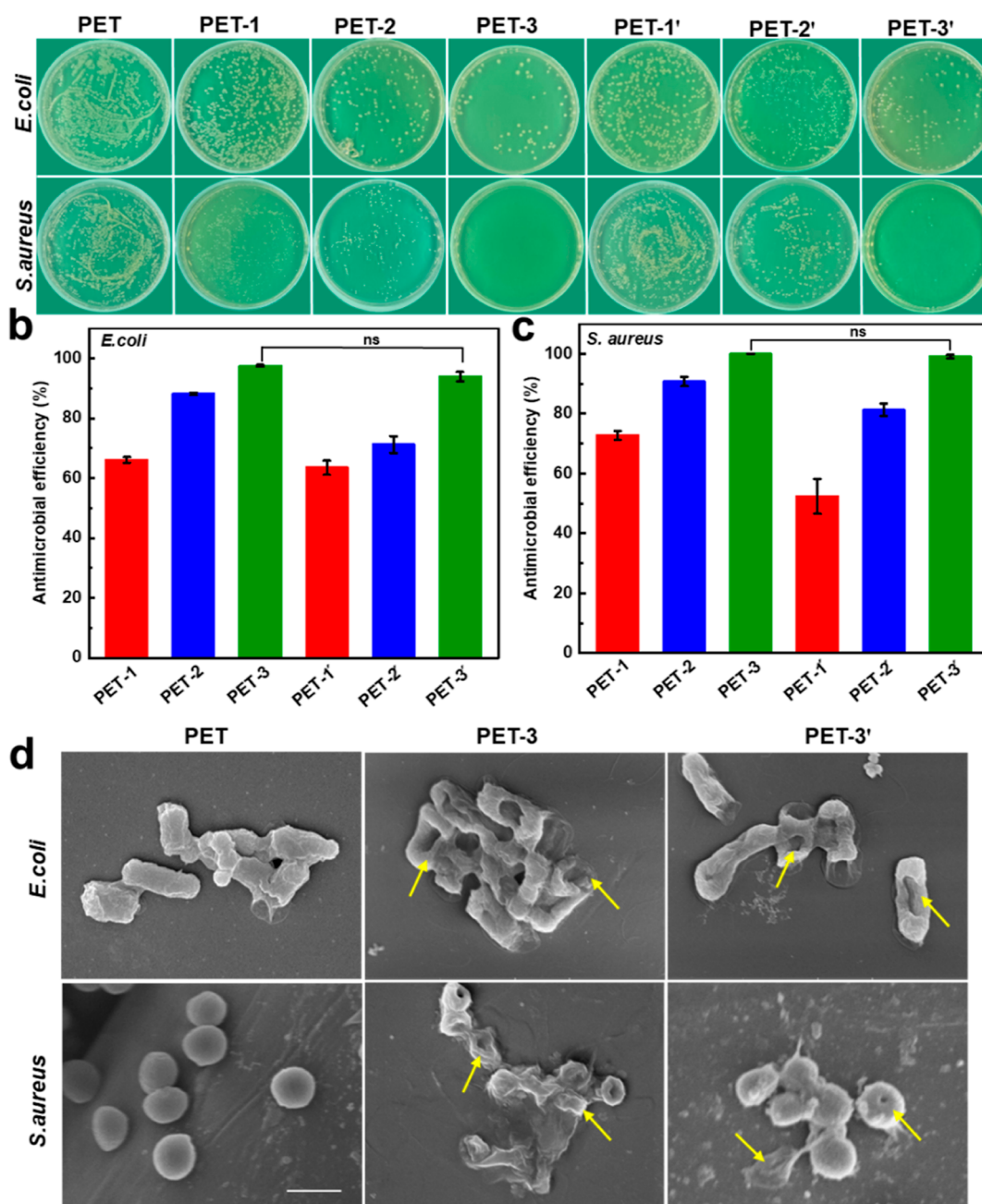


Figure 2. Bactericidal activity of PET and modified PET. (a) Culture medium images of different fabrics. (b) Antimicrobial efficiency of fabrics against *E. coli*. (c) Antimicrobial efficiency of samples against *S. aureus*. (d) SEM images of bacteria after 24 h of direct contact with the fabrics. The scale bar in the image is 1 μm . ns $p > 0.05$.

3. RESULTS AND DISCUSSION

3.1. Preparation and Characterization of the Fabric.

PET was first modified by an ammonolysis reaction (Scheme 1a, Step 1). Under alkali-catalyzed conditions, the amino molecules in PEI were inserted into the chains of PET, leading to the breakage of ester bonds and the formation of amide bonds.¹⁷ PEI was chosen as the solution for the aminolysis reaction because it achieves activation of the inert surface of PET. PEI also plays a bactericidal role as a cation, and its antibacterial activity is closely related to the molecular weight of PEI.³⁸ Subsequently, the amino group on the surface of PET and the aldehyde group on BF are covalently combined by an efficient Schiff base reaction (Scheme 1a, Step 2). Due to the combination of PEI and BF, the modified polyester fabric has

the potential of antimicrobial, food packaging, and accelerated wound healing (Scheme 1b I–III).

PEI with different molecular weights can bring not only different bactericidal abilities to polyester but also different amounts of amino groups to the polyester surface. The number of amino groups will affect the grafting density of the subsequent BF. Therefore, in the first step of polyester modification, we chose three different molecular weight PEIs to carry out the ammonolysis of PET. For PET-1, -2, and -3, the microstructure of the fibers was slightly damaged to different degrees compared to PET. In terms of PET-1', -2', and -3', they showed a color change visible to the naked eye and an increase in microscopic roughness (Figure 1a). The quantitative analysis of the amino density of modified PET was

carried out by orange II staining. Orange II dyes can bind to the amino groups on the surface of the fabric under acidic conditions, and the shade of the color reflects the number of amino groups.³⁹ From the photos after dyeing, PET appeared white due to the absence of amino groups on the surface. With PEI modification, the fabric showed different degrees of orange color visible to the naked eye, with PET-3 having the darkest color. After BF grafting, the color of PET-1', -2', and -3' showed a slight decrease compared to PET-1, -2, and -3 (Figure S2). The amino densities of PET-1, -2, and -3 and PET-1', -2', and -3' were 667.8, 1650.3, 3194.4, 575.1, 1324.3, and 2414.2 $\mu\text{mol/g}$, respectively (Figure 1b). The decrease in the amino density on the sample surface compared to the sample with the previous amino step indicates that BF occupies the amino site. The grafting densities of the BF of PET-1', -2', and -3' can be calculated as 92.7, 326.0, and 780.1 $\mu\text{mol/g}$, respectively. Based on this result, the degree of grafting of BF for PET-1', -2', and -3' is 13.9, 19.7, and 24.4%, respectively. The change in the contact angle of the fabric before and after finishing was also measured (Figure 1c). The WCA of PET changed after the ammonolysis reaction ($\text{CA} = 96 \rightarrow 0^\circ$) because of the strong hydrophilicity of PEI, which was similar to that previously reported.⁴⁰ The WCAs of PET-1', -2', and -3' were above 110° , which was caused by the hydrophobic cage-like structure of BF.

The attenuated total reflection–Fourier-transformed infrared (ATR-FTIR) spectra were used to confirm the changes in characteristic functional groups before and after fabric finishing (Figure 1d). All fabrics showed the C=O stretching of ester groups (1702 cm^{-1}), the deformation of the benzyl group (1099 cm^{-1}), and the C–H out-of-plane bending vibration of benzene (720 cm^{-1}) resulting from the distinctive characteristic peaks of PET. The appearance of amide bond characteristic vibrations (1468 cm^{-1}) and the N–H stretching of primary amines (3300 cm^{-1}) in PET-3 (compared to the ATR-IR spectra of PET) indicated that the aminolysis of PET was successfully carried out. For PET-3', a new characteristic C=N vibrational peak (1636 cm^{-1}) represented the formation of Schiff base bonds.²¹ In addition, the characteristic peaks of amines and hydroxyl groups at 3300 cm^{-1} were not observed in PET-3', which may be due to the apparent decrease in the amount of amines in the fabric.

XPS was also used to confirm the elemental composition of the fabric surface (Figure 1e). PET-3 showed significant changes in C 1s (73.96 wt %), O 1s (6.06 wt %), and N 1s (19.98 wt %) compared with those of PET (73.20 wt %, 25.28 wt %, and 1.52 wt %, respectively) (Table S1). Theoretically, there was no nitrogen on the surface of pure PET, but N appeared in the XPS spectrum. This may be due to other unknown residues on the surface of commercial PET that cannot be cleaned. For PET-3, the C 1s XPS spectrum (Figure S4b) showed three component peaks at 284.8, 285.6, and 288.8 eV, respectively, assigned to C–C/C–H, O–C–C, and C=O. Notably, another component peak can be observed at 285.6 eV, which was closely related to the amide N, indicating abundant amide bonds. In the O 1s XPS spectrum (Figure S4b), a significant peak indexed to O–H (531.4 eV) was presented, owing to the aminolysis reaction. In addition, the N 1s spectrum (Figure S4b) showed two component peaks at 399.3 and 400.1 eV, respectively, assigned to N–C and NH_3^+ . After modification with BF, PET-3' showed significant changes compared with PET-3. Two new components of the C 1s XPS spectrum (Figure S4c) could be observed at 285.0 and 286.2

eV, closely related to the C of the Schiff base bond. Importantly, in the N 1s XPS spectrum (Figure S4c), a major peak indexed to N=C (531.4 eV) was presented owing to the reaction of aldehydes and amino groups.

3.2. Bactericidal Activity Assay. Gram-negative *E. coli* and Gram-positive *S. aureus* were selected to evaluate the biocidal efficacies of the fabrics. PET-1, -2, and -3 exhibited different degrees of killing efficiency against *E. coli* and *S. aureus* (Figure 2a). By electrostatic interaction, the positively charged PEI interferes severely with the bacterial film when bacteria approach the fabric, resulting in the death of the bacteria.⁴¹ In addition, with the increase in molecular weight of PEI, the antibacterial efficiency of PEI-PET against two bacteria kept increasing (Figure 2b,c), indicating a positive correlation between the antimicrobial activity of the cationic polymer and the amino density of PEI. It has been reported that the antibacterial activity of PEI against *E. coli* and *S. aureus* depends on the structure and molecular weight (M_w) of PEI.⁴² In addition, the PEI-modified PET fabrics showed different antibacterial efficiencies against *E. coli* and *S. aureus*. The reason for this phenomenon is that the selective antibacterial activity of PEI against Gram-positive bacteria *S. aureus* is significantly better than that against Gram-negative bacteria *E. coli*.⁴³

The antibacterial activity of PET-1', -2', and -3' decreased in varying degrees after grafting BF, which was due to a slight decrease in cation density on the fabric surface. For example, the antibacterial efficiency of PET-3 against *E. coli* and *S. aureus* reached more than 99.5%. PET-3' showed still high antibacterial efficiency against *E. coli* and *S. aureus* at 93.5 and 99.1%, respectively. The results of the significant difference analysis indicate that although the grafting of BF caused a decrease in the density of cationic groups of PET-3, it did not cause a significant decrease in bactericidal efficiency ($p > 0.05$). This may be because borneol has a rigid structure that allows it to act as a membrane-targeting substance embedded in bacterial membranes, which would somewhat attenuate the effect of cation density reduction on the antibacterial effect.^{24,44}

In order to better understand the antibacterial mechanism of PET-3', the morphological characteristics of the bacteria after contact with the fabric were observed. As shown in Figure 2d, the cellular structure of *E. coli* and *S. aureus* in the untreated PET fabric remains smooth and complete. After 24 h of incubation, most bacteria in PET-3 and PET-3' groups showed membrane damage and sharp contraction, which was mainly due to the strong bactericidal effect of PEI. The assumed action mechanism of PEI as a cationic polymer mainly involves the replacement of divalent cations, which bind the negatively charged surfaces of the lipopolysaccharide network together, thus damaging the outer membrane.⁴⁵ It is also possible that after the outer membrane permeability barrier is destroyed, the cationic group will further penetrate into the inner membrane, causing leakage.⁴⁶

To further confirm the killing mechanism, the ZOI experiment was determined. It is accepted that the ZOI experiment could reflect the susceptibility of bacteria to antimicrobial agents and their antimicrobial mechanism to some extent.⁴⁷ The results of the ZOI experiment of PET-3' showed that it did not produce any inhibition against *E. coli* and *S. aureus* (Figure S5), which indicated that the antimicrobial component of PET-3' had nonleaching proper-

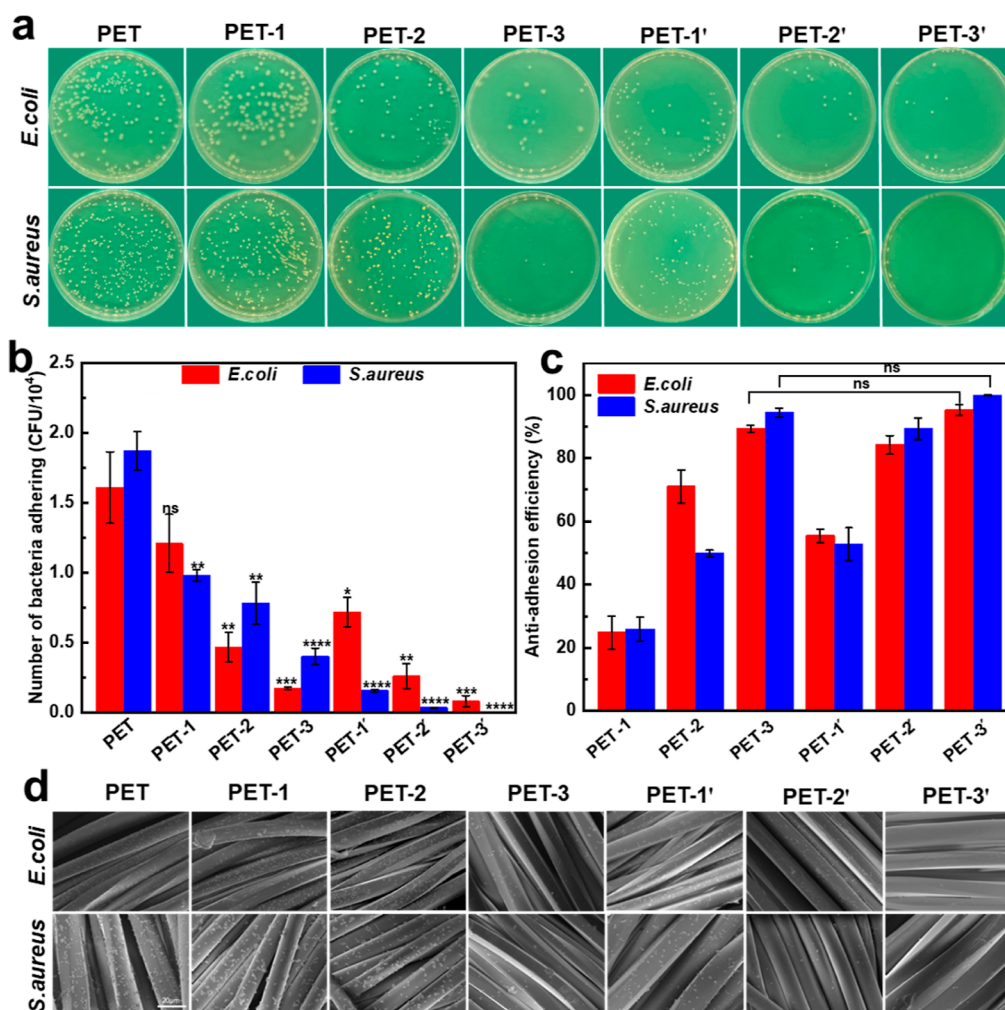


Figure 3. Bacterial adhesion behavior of PET and modified PET. (a) Images of colony counts of bacteria adhering to different fabrics. (b) Statistical numbers of *E. coli* and *S. aureus* adhering to the different fabrics. (c) Antiadhesion efficiency of different fabrics against *E. coli* and *S. aureus*. (d) SEM images of adherent bacteria on control and treated fabrics. The scale bar in the image is 20 μm . **** $p < 0.0001$, *** $p < 0.001$, ** $p < 0.01$, * $p < 0.05$, and ns $p > 0.05$, respectively.

ties. Therefore, the contact killing mechanism was the primary way of PET-3' to exert its antimicrobial function.

3.3. Microbial Adhesion Assay. The surface of the fabric is susceptible to bacterial adhesion to form biofilms, which are difficult to remove.^{48,49} As such, it is imperative that the fabric resists bacterial adhesion effectively. The plate counts showed that PET-1, -2, and -3 exhibited different degrees of adhesion inhibition against *E. coli* and *S. aureus* (Figure 3a). The antiadhesion efficiencies of PET-1, -2, and -3 against *E. coli* were 24.8, 71.0, and 89.3%, respectively. The antiadhesion efficiencies of PET-1, -2, and -3 against *S. aureus* were 25.9, 49.8, and 94.3%, respectively (Figure 3c). Comparing the antibacterial adhesion results of PET modified with different molecular weights of PEI, it is easy to find that PET-3 had the highest antiadhesion activity, well consistent with the results of the biocidal assay. With BF grafting, PET-1', -2', and -3' all exhibited enhanced resistance to bacterial adhesion compared to PET-1, -2, and -3, indicating that the incorporation of BF component into the fabric greatly enhanced the capability to resist bacterial adhesion. This result was contrary to the results of the bactericidal experiment, which was attributed to the unique cage-like monoterpene structure of the borneol monomer. It was deduced that the borneol component on

the fabric enhances resistance to bacterial adhesion by discouraging bacteria from adhering to the fabric surface at the initial stage of adhesion due to the recognition of the "chiral taste".²⁶ Microscopic images of the fabric after contact with the bacterial solution were used to verify this result. The results of SEM showed that a large number of *E. coli* and *S. aureus* adhered to the surface of the PET fabric. The adherence of bacteria on PET-1, -2, and -3 showed different degrees of decrease with different PEI modifications. It can be observed that there is still a small number of bacteria adhering to the surface of the PET-3 fabric. Compared to PET-1, -2, and -3, there was a significant decrease in bacteria adhered to PET-1', -2', and -3'. The PET-3' fabric was very smooth, and no bacterial adhesion was observed (Figure 3d). Thus, the combination of the bactericidal effect of PEI and the antiadhesive effect of BF endowed PET fabrics with good resistance to bacterial adhesion.

3.4. Fungal Repelling Assay. The resistance of polyesters to fungal adhesion was evaluated by visualizing an experimental model of fungal repulsion.⁵⁰ The model is based on the selection of *A. niger* and *M. racemosus*, and the incubation time is 30 d. *A. niger* or *M. racemosus* spreads in a circular pattern from the center to the periphery of the medium, and when it

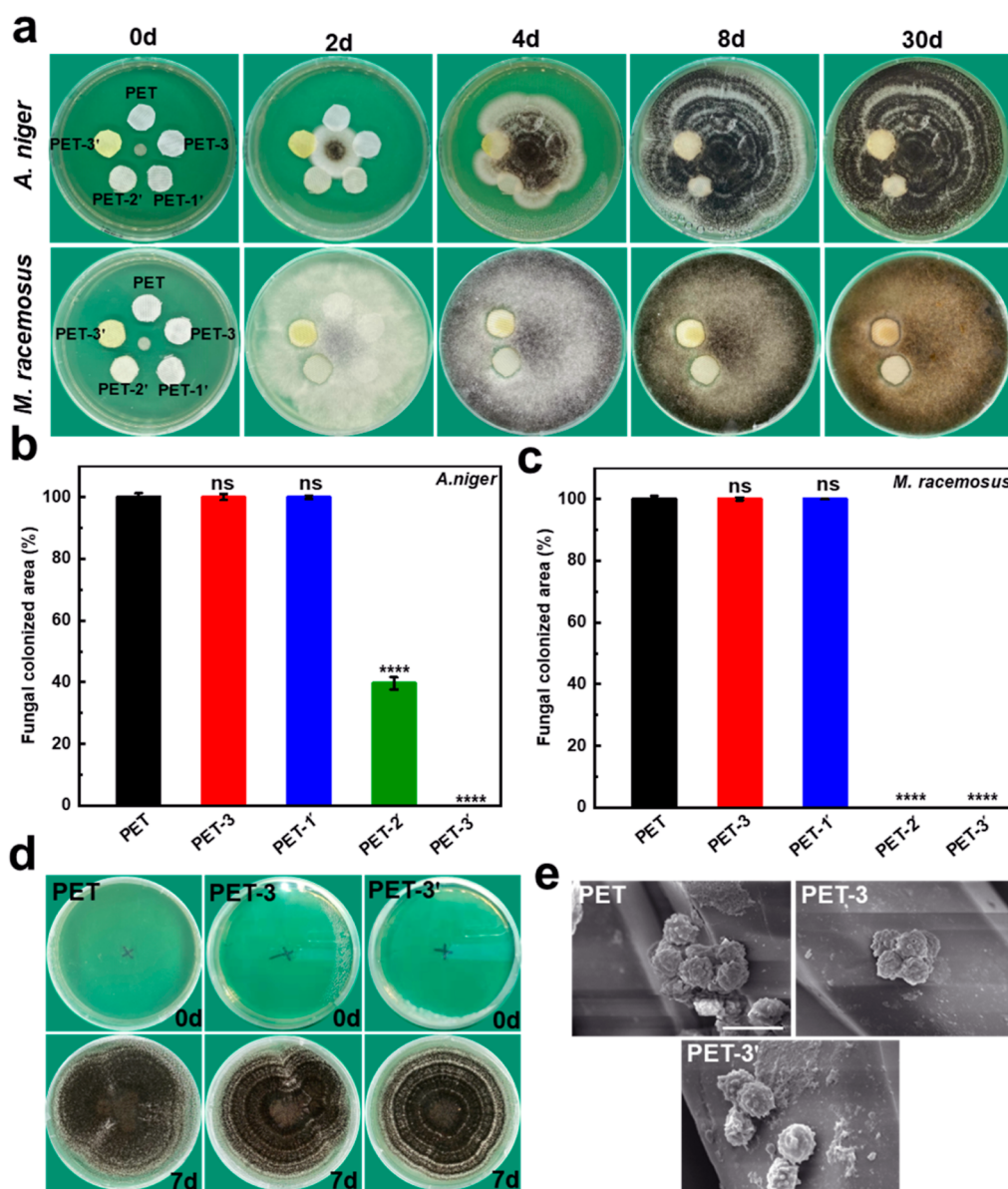


Figure 4. Fungal repulsion behavior of PET and modified PET. (a) Digital photos of the fungal (*A. niger* and *M. racemosus*) repulsion effect of the fabrics in 30 d. (b) Quantification of fungal colonization areas on the surface of fabrics against *A. niger*. (c) Quantification of fungal colonization areas on the surface of fabrics against *M. racemosus*. (d) Digital photos of the "stamp" experiment. (e) SEM images of *A. niger* after 24 h of direct contact with the fabric. The scale bar in the image is 5 μm . **** $p < 0.0001$, and ns $p > 0.05$.

touches the edge of the material, it can choose to climb up or around the material and continue to grow, thus determining whether the material can resist fungal adhesion.

Considering that PET-1, -2, and -3 had been proven to kill bacteria in varying degrees (Figure 2), we first verified whether they could also be resistant to fungal adhesion. Unfortunately, PET-1, -2, and -3 showed poor antifungal effects. In antifungal landing experiments, all three samples were completely covered by *A. niger* and *M. racemosus*, indicating the samples had no resistance effect to fungal contamination (Figure S6). As shown in Figure 4a, the surfaces of PET, PET-3, and PET-1' fabrics were gradually covered with black *A. niger* or *M. racemosus*, while no black *A. niger* or *M. racemosus* was observed on the surface of PET-2' and PET-3' fabrics. Upon magnification of the fabric (Figure S7), numerous fungal (*A. niger* or *M. racemosus*) overlays could be observed on the PET, PET-3, and PET-1' surfaces; in contrast, PET-2' and PET-3'

exhibited clear surfaces without any fungal stains and produced distinct edges of growth inhibition. Quantitative statistical studies of fungal adhesion to the material surface were performed by Image J software; PET-1' was covered by *A. niger* and *M. racemosus* with almost 100% coverage in 8 d. On the contrary, PET-3' showed good antiadhesive properties against both *A. niger* and *M. racemosus* with a coverage rate close to 0% in 30 d (Figure 4b,c). This was because the unique stereochemical structure of BF gave the fabric good fungal repelling properties. In addition, the performance of PET-2' in the antifungal evaluation was worth exploring. In the anti-*A. niger* experiment, PET-2' showed a degree of antifungal effect after 30 d, when *A. niger* appeared partially covered on the material's surface, with a surface coverage of about 40%. This result is similar to previous reports that the antibacterial effect of borneol-modified surfaces is closely related to the density of small molecules.^{32,51,52} Therefore, compared with PET-1', the

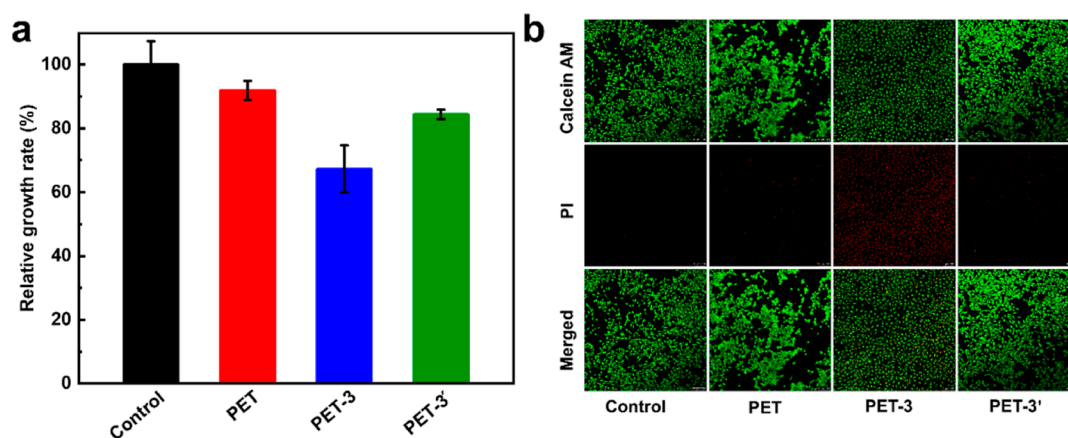


Figure 5. Cytotoxicity of PET and modified PET. (a) Relative growth rates of L929 cells after 48 h of incubation with the fabrics. (b) Fluorescence microscopy images of L929 cells after 48 h of incubation with the fabrics. The scale bar in the image is 100 μm .

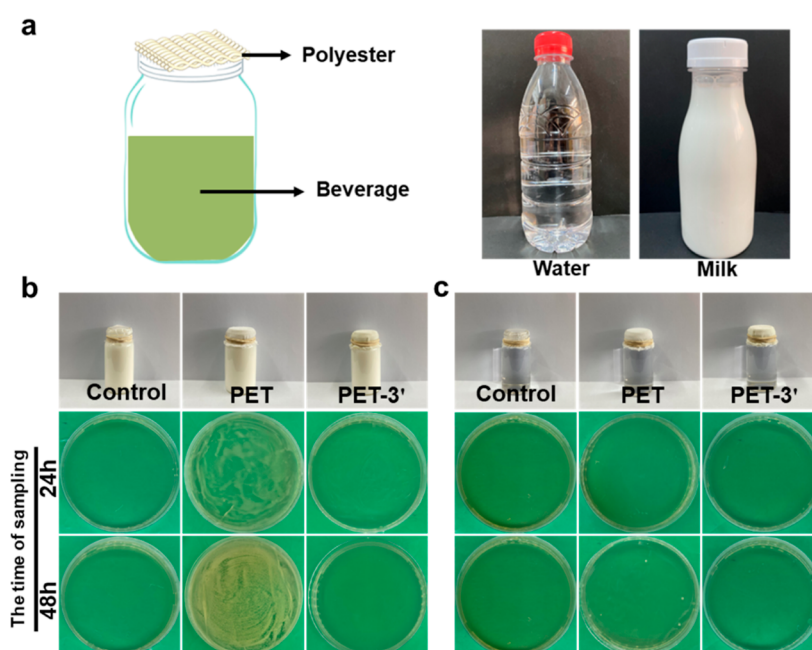


Figure 6. Photographic images of food preservation. (a) Schematic diagram of food preservation experiment and commercial beverage. (b) Inactivated milk and (c) water, 100 μL , on the TSA plate, sampling after 24 and 48 h storage, respectively.

anti-*A. niger* effect of PET-2' improved but did not reach the expected effect (Figure 4b). In the anti-*M. racemosus* experiment, PET-2' remained clean after 30 d (Figure 4c). The difference in the degree of contamination of PET-2 against these two different types of fungi may be due to the different sensitivities of different classes of fungi to borneol.

In addition, to explore whether PET-3 can kill fungal spores, a simple "contact-killing" sandwich structure was designed. After 24 h of contact between spores and the material, the material with spores was brought into full contact with the medium, and then it could be judged whether the material had killed the spores by observing whether there was fungal growth on the medium. After 7 d, it was observed that all three groups had *A. niger* growing on the medium (Figure 4d). In addition, the microscopic morphology of *A. niger* spores after contact with the fabric was also observed to determine whether the three fabrics had a membrane-disrupting effect on the fungi (Figure 4e). The results showed that all groups of *A. niger* spores did not show cell lysis or membrane deformation and

invagination, which indicated that all three fabrics could not kill *A. niger* spores. This phenomenon may be due to the thick outer membrane of the fungus and its low density of negatively charged lipids,⁵³ which prevented the effective breaking and killing of both PET-3 and PET-3' against *A. niger*. Therefore, PET-3' can protect from fungal contamination by repelling the fungi rather than killing them.

3.5. Cytotoxicity Assay. Cytotoxicity is a crucial indicator in assessing the biocompatibility of antimicrobial fabrics. Thus, the cytotoxicity of PET-3' fabrics with the best antimicrobial performance was evaluated according to standard MTT methods. The results were expressed as relative percentages of negative controls (100% cell viability). As shown in Figure 5a, the cell viability of PET was maintained at $91.9 \pm 3.0\%$ while that of PET-3 was only $67.3 \pm 7.3\%$, which proves that the presence of a large number of cationic groups of high-molecular-weight PEI resulted in the killing of cells. Notably, compared to PET-3, there was a significant increase in cell viability in PET-3' remaining at $84.4 \pm 1.5\%$, suggesting that

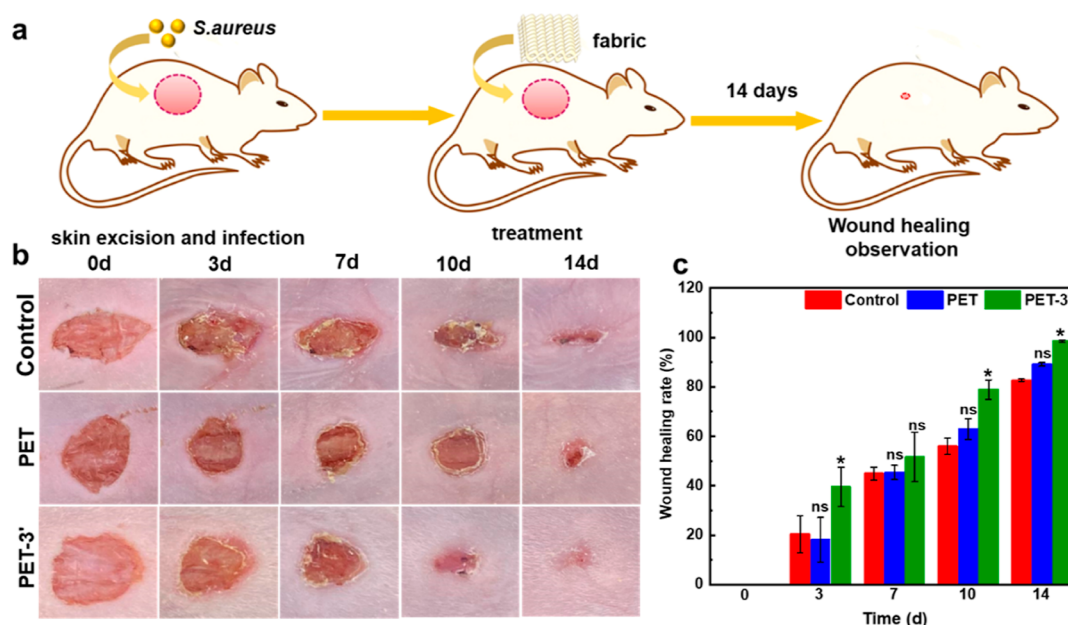


Figure 7. Study of In vitro wound healing. (a) Schematic representation of wounds and treatment regimen in rats. (b) Representative photographs of wounds infected with *S. aureus* and treated with different methods from 0 to 14 d. (c) Quantitative residual wound percentage statistics from day 0 to 14 d. Data are reported as means \pm SD. * $p < 0.05$ and ns $p > 0.05$.

the BF modification reduced the cytotoxicity of PEI.⁵⁴ According to the standard toxicity rating in the Pharmacopoeia of the United States (USP, Table S2), the cytotoxicity of PET-3' is in grade 1 (Table S3). Fluorescence microscopy images were further used to confirm the state of the cells. As shown in Figure 5b, the cell populations in PET and PET-3' showed high viability, and the cells retained their spindle-shaped morphology. In contrast, the cell population in the PET-3 group showed significant deformation. This result corresponds to the MTT results. Thus, PET-3' is an antimicrobial fabric with low cytotoxicity.

3.6. Application of Food Preservation. A simple experiment was designed to verify the potential of polyesters in food preservation (Figure 6a). Water and milk were chosen as the subjects of the study. Commercially available milk and sterile water are usually sterile. The special sealing film selected in the control group was able to isolate the entry of microorganisms, so almost no airborne microorganisms were able to enter the control bottles and no bacterial colonies were observed on the TSA plate throughout the incubation process (Figure 6b). After 24 h of storage, the milk from the PET group contained bacteria, as evidenced by visible colonies growing on the TSA plate, indicating that the milk had been contaminated with bacteria during storage. In contrast, bacterial colonies did not appear in the TSA plate of the aliquots of milk from the PET-3' group until 48 h (Figure 6b). On the other hand, within 48 h, almost no bacterial colonies were observed on the Petri dishes of the water samples in the PET-3' group; in contrast, a small number of bacterial colonies appeared in the PET-3 group (Figure 6c). The percentages of bacterial colonies in the plates of different groups were quantified by ImageJ (Figure S8). The results showed that the plates of the PET-3' group had significantly lower bacterial colonies than those of the PET-3 group after 48 h of storage of milk and water ($p < 0.0001$). This phenomenon indicated that PET-3' effectively blocked the entry of airborne bacteria due to its good antibacterial properties.

3.7. Application of Wound Healing. To evaluate the therapeutic effect of the PET-3' fabric on infected wounds in vivo, a mouse whole-skin tissue wound infection model was constructed using *S. aureus* at a concentration of 10^8 CFU/mL to simulate infected wounds (Figure 7a). The wound healing efficiency of PET-3' fabric was evaluated by observing the wound surface morphology and calculating the wound area percentage results. The blank group was not treated except for bacterial infection. The wounds in all groups showed a gradual decrease and reduction over time (Figure 7b). However, at any of the periods (3, 7, 10, and 14 d), the wound healing rate was significantly faster in the PET-3' group than in the PET and control groups. The calculated residual wound percentages shown in Figure 7c quantitatively demonstrate the significant therapeutic effect of PET-3' on the healing of infected wounds compared to the PET and control groups. Specifically, the wound healing rate in the PET-3' group reached 39.5 ± 8.0 , 51.6 ± 10.1 , 78.9 ± 3.9 , and $98.4 \pm 0.5\%$ on 3, 7, 10, and 14 d, respectively, compared to 18.1 ± 9.0 , 45.3 ± 2.8 , 62.9 ± 4.2 , and $89.2 \pm 0.7\%$ in the PET group. All results indicated that PET-3' accelerates wound healing, which is attributed to the combination of the cationic bactericidal and stereochemical antiadhesive properties of PET-3' fabrics. On the one hand, the cationic polymer PEI is effective in killing bacteria during contact with the wound due to its powerful bactericidal effect.⁴⁵ On the other hand, the stereochemical structure of the borneol can effectively prevent the adhesion of harmful microorganisms in the air.²¹ In addition, the structure of the PEI-finished fabric becomes looser compared to the original PET fabric, and the loose structure results in higher water vapor permeability (Figure S9). This structural feature contributes to the need for air–fluid exchange in the wound, thus promoting wound healing.⁵⁵ Therefore, the PET-3' fabric has great potential in promoting wound healing, especially bacterial infection wound healing.

3.8. Mechanical Properties and Washing Durability. The aminolysis reaction of PET often leads to the breakage of

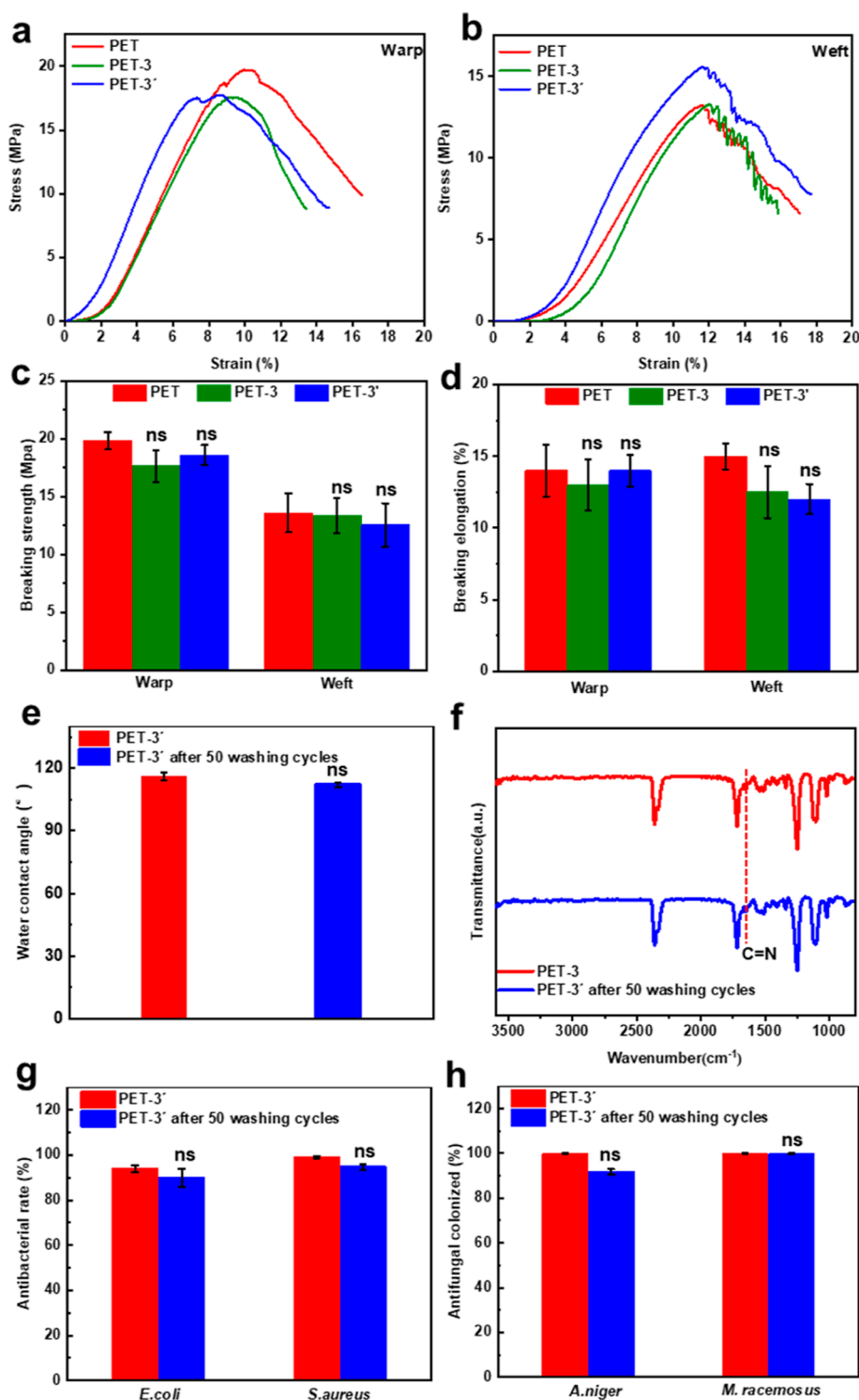


Figure 8. Mechanical properties and washing durability of PET and modified PET. (a,b) Stress–strain curves of PET, PET-3, and PET-3'. (c) Breaking strength and (d) breaking elongation of PET, PET-3, and PET-3'. (e) WCA of PET-3' before and after 50 washing cycles. (f) ATR-FTIR survey spectra of PET-3' before and after 50 washing cycles. (g) Antibacterial efficiency of PET-3' after 50 washing cycles. (h) Fungal repelling properties of PET-3' after 50 washing cycles. ns $p > 0.05$.

the polymer chain of PET, causing a decrease in the mechanical properties of the fabric.⁵⁶ Therefore, it is essential that the mechanical properties of the modified PET fabric can meet daily requirements. As expected, the mechanical property of PET-3 and PET-3' was somewhat degraded compared to PET (Figure 8a,b). The breaking strength of PET-3' decreased from 19.8 ± 0.75 to 18.6 ± 0.85 MPa in the warp direction and

from 13.6 ± 1.7 to 12.5 ± 1.9 MPa in the weft direction and the elongation at break increased from 14.0 ± 1.8 to $14.0 \pm 1.1\%$ in the warp direction and from 15.0 ± 0.9 to $12.0 \pm 1.0\%$ in the weft direction (Figure 8c,d). The results of the statistical analysis showed that there was no significant difference in the breaking strength and elongation at break of the three fabrics

($p > 0.05$). Thus, the modified fabric still maintains good mechanical properties.

Washing durability is an important feature to evaluate the reusability of the developed antimicrobial fabrics.⁵⁷ After 50 repeated washing cycles, the hydrophobic performance of PET-3' remained stable, and the WCA was maintained at 116° (Figure 8e). Proper hydrophobicity ensured that the fabric can be used for medical protective materials such as medical-surgical masks and protective clothing with waterproof requirements.⁶ The surface chemical structure of PET-3' after washing was reviewed by ATR-FTIR spectroscopy (Figure 8f). Similar ATR-FTIR spectra of PET-3' before and after 50 wash cycles showed no change in the molecular structure. The characteristic absorption peaks of the Schiff base structure at 1720 cm⁻¹ (C=O vibration) and 1636 cm⁻¹ (C=N vibration) were still present. The washing durability of PET-3' came from the excellent stability of the hydrophobic Schiff base structure, which stabilizes the Schiff base even under weakly acidic conditions.^{58,59} In addition, previous reports from our group had shown that most detergents were alkaline.²¹ Therefore, PET-3' Schiff base was strong enough to survive the action of common detergents, thus providing stable modification and long-lasting antimicrobial ability. Based on the antimicrobial effect, PET-3' was selected as the characteristic antimicrobial fabric to test its reusability. After 50 washing cycles, the antibacterial activity of PET-3' against *E. coli* and *S. aureus* was maintained at 90.1 ± 4.0 and 94.7 ± 1.3%. The antibacterial activity of PET-3 was maintained at 91.1 ± 1.5 and 94.8 ± 0.8% (Figures 8g and S11). The antibacterial activity of PET-3 and PET-3' did not show significant differences after washing ($p > 0.05$). Also, the antifungal (*A. niger* and *M. racemosus*) coverage area of PET-3' was 91.8 ± 1.2 and 99.8 ± 0.1% (Figures 8h and S12). Therefore, PET-3' has good washing durability.

4. CONCLUSIONS

In summary, a PET fabric with diversiform antimicrobial abilities was prepared using the cationic polymer PEI and stereochemical borneol based on an "integrated attack and defense" strategy. The dual coordination between borneol and PEI endowed PET fabric with a high bactericidal effect, good antifungal performance, and acceptable biocompatibility. The results of two simple models for practical applications showed that the fabric had great potential for applications in food storage and in preventing wound infection and promoting wound healing. In particular, the introduction of the stereochemical borneol not only effectively compensated for the lack of antifungal ability of the traditional cationic PEI but also improved the biocompatibility of the final finished materials. Besides, the bactericidal properties of conventional cations were maintained and did not change or disappear as a result. In other words, the traditional cationic PEI also endowed the bactericidal ability which the stereochemical antimicrobial strategy lacked. Therefore, it is optimistic to anticipate that the dual coordination between stereochemical components and traditional antimicrobial components such as quaternary ammonium salts, zwitterionic compounds, polyethylene glycols, and nanoparticles will also be a win-win outcome.

■ ASSOCIATED CONTENT

Supporting Information

The Supporting Information is available free of charge at <https://pubs.acs.org/doi/10.1021/acsami.2c19323>.

Synthesis route and ¹H NMR of BF; photograph of fabrics dyed with orange II; CA of fabrics; high-resolution XPS of fabrics; ZOI experiment of PET-3'; fungal landing test of PET-1, PET-2, and PET-3; water vapor permeability of PET, PET-3, and PET-3'; MTT results of the fabrics; quantitative results of food preservation experiments; and antibacterial and fungal repelling results of PET-3 and PET-3' after 50 washing cycles (PDF)

■ AUTHOR INFORMATION

Corresponding Author

Xing Wang – State Key Laboratory of Organic-Inorganic Composites; Beijing Laboratory of Biomedical Materials; College of Life Science and Technology, Beijing University of Chemical Technology, Beijing 100029, P. R. China; orcid.org/0000-0002-9990-1479; Email: wangxing@mail.buct.edu.cn

Authors

Pengfei Zhang – State Key Laboratory of Organic-Inorganic Composites; Beijing Laboratory of Biomedical Materials; College of Life Science and Technology, Beijing University of Chemical Technology, Beijing 100029, P. R. China

Xinyu Chen – State Key Laboratory of Organic-Inorganic Composites; Beijing Laboratory of Biomedical Materials; College of Life Science and Technology, Beijing University of Chemical Technology, Beijing 100029, P. R. China

Fanqiang Bu – State Key Laboratory of Organic-Inorganic Composites; Beijing Laboratory of Biomedical Materials; College of Life Science and Technology, Beijing University of Chemical Technology, Beijing 100029, P. R. China

Chen Chen – State Key Laboratory of Organic-Inorganic Composites; Beijing Laboratory of Biomedical Materials; College of Life Science and Technology, Beijing University of Chemical Technology, Beijing 100029, P. R. China

Lifei Huang – State Key Laboratory of Organic-Inorganic Composites; Beijing Laboratory of Biomedical Materials; College of Life Science and Technology, Beijing University of Chemical Technology, Beijing 100029, P. R. China

Zixu Xie – State Key Laboratory of Organic-Inorganic Composites; Beijing Laboratory of Biomedical Materials; College of Life Science and Technology, Beijing University of Chemical Technology, Beijing 100029, P. R. China

Guofeng Li – State Key Laboratory of Organic-Inorganic Composites; Beijing Laboratory of Biomedical Materials; College of Life Science and Technology, Beijing University of Chemical Technology, Beijing 100029, P. R. China;

orcid.org/0000-0002-4101-0059

Complete contact information is available at: <https://pubs.acs.org/doi/10.1021/acsami.2c19323>

Notes

The authors declare no competing financial interest.

■ ACKNOWLEDGMENTS

The authors thank the National Natural Science Foundation of China (52273118, 22275013, and 21574008) for financial

support. Some of the images in the TOC were obtained from Vecteezy.com.

REFERENCES

- (1) Zhang, S.; Li, R.; Huang, D.; Ren, X.; Huang, T. S. Antibacterial Modification of PET with Quaternary Ammonium Salt and Silver Particles via Electron-Beam Irradiation. *Mater. Sci. Eng. C* **2018**, *85*, 123–129.
- (2) Gupta, P.; Bairagi, N.; Priyadarshini, R.; Singh, A.; Chauhan, D.; Gupta, D. Bacterial Contamination of Nurses' White Coats Made from Polyester and Polyester Cotton Blend Fabrics. *J. Hosp. Infect.* **2016**, *94*, 92–94.
- (3) Yang, R.; Wang, X.; Yan, S.; Dong, A.; Luan, S.; Yin, J. Advances in Design and Biomedical Application of Hierarchical Polymer Brushes. *Prog. Polym. Sci.* **2021**, *118*, 101409.
- (4) Dong, A.; Wang, Y.-J.; Gao, Y.; Gao, T.; Gao, G. Chemical Insights into Antibacterial N-Halamines. *Chem. Rev.* **2017**, *117*, 4806–4862.
- (5) Zou, Y.; Zhang, Y.; Yu, Q.; Chen, H. Dual-Function Antibacterial Surfaces to Resist and Kill Bacteria: Painting a Picture with Two Brushes Simultaneously. *J. Mater. Sci. Technol.* **2021**, *70*, 24–38.
- (6) Wang, S.; Li, J.; Cao, Y.; Gu, J.; Wang, Y.; Chen, S. Non-Leaching, Rapid Bactericidal and Biocompatible Polyester Fabrics Finished with Benzophenone Terminated N-Halamine. *Adv. Fiber Mater.* **2021**, *4*, 119.
- (7) Wang, Y.; Xia, G.; Yu, H.; Qian, B.; Cheung, Y. H.; Wong, L. H.; Xin, J. H. Mussel-Inspired Design of a Self-Adhesive Agent for Durable Moisture Management and Bacterial Inhibition on PET Fabric. *Adv. Mater.* **2021**, *33*, 2100140.
- (8) Hasan, K. M. F.; Pervez, Md. N.; Talukder, Md. E.; Sultana, M. Z.; Mahmud, S.; Meraz, Md. M.; Bansal, V.; Genyang, C. A Novel Coloration of Polyester Fabric through Green Silver Nanoparticles (G-AgNPs@PET). *Nanomaterials* **2019**, *9*, 569.
- (9) Quartinello, F.; Tallian, C.; Auer, J.; Schön, H.; Vielnascher, R.; Weinberger, S.; Wieland, K.; Weihs, A. M.; Herrero-Rollet, A.; Lendl, B.; Teuschl, A. H.; Pellis, A.; Guebitz, G. M. Smart Textiles in Wound Care: Functionalization of Cotton/PET Blends with Antimicrobial Nanocapsules. *J. Mater. Chem. B* **2019**, *7*, 6592–6603.
- (10) Zhai, W.; Cao, Y.; Li, Y.; Zheng, M.; Wang, Z. MoO₃-x QDs/MXene (Ti₃C₂T_x) Self-Assembled Heterostructure for Multifunctional Application with Antistatic, Smoke Suppression, and Antibacterial on Polyester Fabric. *J. Mater. Sci.* **2022**, *57*, 2597–2609.
- (11) Xu, J.; Kerr, L.; Jiang, Y.; Suo, W.; Zhang, L.; Lao, T.; Chen, Y.; Zhang, Y. Rapid Antigen Diagnostics as Frontline Testing in the COVID-19 Pandemic. *Small Sci.* **2022**, *2*, 2200009.
- (12) Cheng, D.; Lin, X.; Fan, L.; Cai, G.; Wu, J.; Yu, W. Preparation and Characterization of Polyelectrolyte/Silver Multilayer Films on PET Substrates and Its Antibacterial Property. *Polym. Compos.* **2015**, *36*, 1161–1168.
- (13) Xin, X.; Li, P.; Zhu, Y.; Shi, L.; Yuan, J.; Shen, J. Mussel-Inspired Surface Functionalization of PET with Zwitterions and Silver Nanoparticles for the Dual-Enhanced Antifouling and Antibacterial Properties. *Langmuir* **2019**, *35*, 1788–1797.
- (14) Lv, J.; Zhou, Q.; Zhi, T.; Gao, D.; Wang, C. Environmentally Friendly Surface Modification of Polyethylene Terephthalate (PET) Fabric by Low-Temperature Oxygen Plasma and Carboxymethyl Chitosan. *J. Cleaner Prod.* **2016**, *118*, 187–196.
- (15) Ping, X.; Wang, M.; Xuewu, G. Surface Modification of Poly(Ethylene Terephthalate) (PET) Film by Gamma-Ray Induced Grafting of Poly(Acrylic Acid) and Its Application in Antibacterial Hybrid Film. *Radiat. Phys. Chem.* **2011**, *80*, 567–572.
- (16) Chen, S.; Zhang, S.; Galluzzi, M.; Li, F.; Zhang, X.; Yang, X.; Liu, X.; Cai, X.; Zhu, X.; Du, B.; Li, J.; Huang, P. Insight into Multifunctional Polyester Fabrics Finished by One-Step Eco-Friendly Strategy. *Chem. Eng. J.* **2019**, *358*, 634–642.
- (17) Lorusso, E.; Feng, Y.; Schneider, J.; Kamps, L.; Parasothy, N.; Mayer-Gall, T.; Gutmann, J. S.; Ali, W. Investigation of Aminolysis Routes on PET Fabrics Using Different Amine-Based Materials. *Nano Sel.* **2022**, *3*, 594–607.
- (18) Lin, J.; Qiu, S.; Lewis, K.; Klivanov, A. M. Mechanism of Bactericidal and Fungicidal Activities of Textiles Covalently Modified with Alkylated Polyethylenimine. *Biotechnol. Bioeng.* **2003**, *83*, 168–172.
- (19) Hook, A. L.; Chang, C.-Y.; Yang, J.; Luckett, J.; Cockayne, A.; Atkinson, S.; Mei, Y.; Bayston, R.; Irvine, D. J.; Langer, R.; Anderson, D. G.; Williams, P.; Davies, M. C.; Alexander, M. R. Combinatorial Discovery of Polymers Resistant to Bacterial Attachment. *Nat. Biotechnol.* **2012**, *30*, 868–875.
- (20) Ma, Y.; Shi, L.; Yue, H.; Gao, X. Recognition at Chiral Interfaces: From Molecules to Cells. *Colloids Surf., B* **2020**, *195*, 111268.
- (21) Xu, J.; Zhao, H.; Xie, Z.; Ruppel, S.; Zhou, X.; Chen, S.; Liang, J. F.; Wang, X. Stereochemical Strategy Advances Microbially Antiadhesive Cotton Textile in Safeguarding Skin Flora. *Adv. Healthcare Mater.* **2019**, *8*, 1900232.
- (22) Huang, L.; Liu, C.-J. Progress for the Development of Antibacterial Surface Based on Surface Modification Technology. *Supramol. Mater.* **2022**, *1*, 100008.
- (23) Luo, L.; Li, G.; Luan, D.; Yuan, Q.; Wei, Y.; Wang, X. Antibacterial Adhesion of Borneol-Based Polymer via Surface Chiral Stereochemistry. *ACS Appl. Mater. Interfaces* **2014**, *6*, 19371–19377.
- (24) Yang, L.; Zhan, C.; Huang, X.; Hong, L.; Fang, L.; Wang, W.; Su, J. Durable Antibacterial Cotton Fabrics Based on Natural Borneol-Derived Anti-MRSA Agents. *Adv. Healthcare Mater.* **2020**, *9*, 2000186.
- (25) Song, F.; Zhang, L.; Chen, R.; Liu, Q.; Liu, J.; Yu, J.; Liu, P.; Duan, J.; Wang, J. Bioinspired Durable Antibacterial and Antifouling Coatings Based on Borneol Fluorinated Polymers: Demonstrating Direct Evidence of Antiadhesion. *ACS Appl. Mater. Interfaces* **2021**, *13*, 33417–33426.
- (26) Cheng, Q.; Asha, A. B.; Liu, Y.; Peng, Y. Y.; Diaz-Dussan, D.; Shi, Z.; Cui, Z.; Narain, R. Antifouling and Antibacterial Polymer-Coated Surfaces Based on the Combined Effect of Zwitterions and the Natural Borneol. *ACS Appl. Mater. Interfaces* **2021**, *13*, 9006–9014.
- (27) Cheng, Q.; Peng, Y.-Y.; Asha, A. B.; Zhang, L.; Li, J.; Shi, Z.; Cui, Z.; Narain, R. Construction of Antibacterial Adhesion Surfaces Based on Bioinspired Borneol-Containing Glycopolymers. *Biomater. Sci.* **2022**, *10*, 1787–1794.
- (28) Zhang, S.; Yang, X.; Tang, B.; Yuan, L.; Wang, K.; Liu, X.; Zhu, X.; Li, J.; Ge, Z.; Chen, S. New Insights into Synergistic Antimicrobial and Antifouling Cotton Fabrics via Dually Finished with Quaternary Ammonium Salt and Zwitterionic Sulfobetaine. *Chem. Eng. J.* **2018**, *336*, 123–132.
- (29) Xin, Y.; Zhao, H.; Xu, J.; Xie, Z.; Li, G.; Gan, Z.; Wang, X. Borneol-Modified Chitosan: Antimicrobial Adhesion Properties and Application in Skin Flora Protection. *Carbohydr. Polym.* **2020**, *228*, 115378.
- (30) Kumar, P.; Roy, S.; Sarkar, A.; Jaiswal, A. Reusable MoS₂-Modified Antibacterial Fabrics with Photothermal Disinfection Properties for Repurposing of Personal Protective Masks. *ACS Appl. Mater. Interfaces* **2021**, *13*, 12912–12927.
- (31) Song, L.; Sun, L.; Zhao, J.; Wang, X.; Yin, J.; Luan, S.; Ming, W. Synergistic Superhydrophobic and Photodynamic Cotton Textiles with Remarkable Antibacterial Activities. *ACS Appl. Bio Mater.* **2019**, *2*, 2756–2765.
- (32) Zhang, P.; Li, J.; Yang, M.; Huang, L.; Bu, F.; Xie, Z.; Li, G.; Wang, X. Inserting Menthoxytriazine into Poly(Ethylene Terephthalate) for Inhibiting Microbial Adhesion. *ACS Biomater. Sci. Eng.* **2021**, *8*, 570.
- (33) Xu, J.; Xie, Z.; Du, F.; Wang, X. One-Step Anti-Superbug Finishing of Cotton Textiles with Dopamine-Menthol. *J. Mater. Sci. Technol.* **2021**, *69*, 79–88.
- (34) Lu, Z.; Wu, Y.; Cong, Z.; Qian, Y.; Wu, X.; Shao, N.; Qiao, Z.; Zhang, H.; She, Y.; Chen, K.; Xiang, H.; Sun, B.; Yu, Q.; Yuan, Y.; Lin, H.; Zhu, M.; Liu, R. Effective and Biocompatible Antibacterial

Surfaces via Facile Synthesis and Surface Modification of Peptide Polymers. *Bioact. Mater.* **2021**, *6*, 4531–4541.

(35) Wang, L.; Du, L.; Wang, M.; Wang, X.; Tian, S.; Chen, Y.; Wang, X.; Zhang, J.; Nie, J.; Ma, G. Chitosan for Constructing Stable Polymer-Inorganic Suspensions and Multifunctional Membranes for Wound Healing. *Carbohydr. Polym.* **2022**, *285*, 119209.

(36) Li, L.; Wang, W.; Lian, L.; Hu, H.; Wang, W. Antimicrobial Rubber Nanocapsule-Based Iodophor Promotes Wound Healing. *CCS Chem.* **2020**, *2*, 245–256.

(37) Zheng, K.; Tong, Y.; Zhang, S.; He, R.; Xiao, L.; Iqbal, Z.; Zhang, Y.; Gao, J.; Zhang, L.; Jiang, L.; Li, Y. Flexible Bicolorimetric Polyacrylamide/Chitosan Hydrogels for Smart Real-Time Monitoring and Promotion of Wound Healing. *Adv. Funct. Mater.* **2021**, *31*, 2102599.

(38) Bech, L.; Meylheuc, T.; Lepoittevin, B.; Roger, P. Chemical Surface Modification of Poly(Ethylene Terephthalate) Fibers by Aminolysis and Grafting of Carbohydrates. *J. Polym. Sci., Part A: Polym. Chem.* **2007**, *45*, 2172–2183.

(39) Maaz, M.; Elzein, T.; Bejjani, A.; Barroca-Aubry, N.; Lepoittevin, B.; Drago, D.; Mazerat, S.; Nsouli, B.; Roger, P. Surface Initiated Supplemental Activator and Reducing Agent Atom Transfer Radical Polymerization (SI-SARA-ATRP) of 4-Vinylpyridine on Poly(Ethylene Terephthalate). *J. Colloid Interface Sci.* **2017**, *500*, 69–78.

(40) Chen, Y.; Wu, X.; Wei, J.; Wu, H. Nondestructive Modification of Catechol/Polyethyleneimine onto Polyester Fabrics by Mussel-Inspiration for Improving Interfacial Performance. *Macromol. Mater. Eng.* **2020**, *305*, 2000258.

(41) Sinclair, T. R.; Robles, D.; Raza, B.; van den Hengel, S.; Rutjes, S. A.; de Roda Husman, A. M.; de Grooth, J.; de Vos, W. M.; Roesink, H. D. W. Virus Reduction through Microfiltration Membranes Modified with a Cationic Polymer for Drinking Water Applications. *Colloids Surf., A* **2018**, *551*, 33–41.

(42) Song, F.; Wang, J.; Zhang, L.; Chen, R.; Liu, Q.; Liu, J.; Yu, J.; Liu, P.; Duan, J. Synergistically Improved Antifouling Efficiency of a Bioinspired Self-Renewing Interface via a Borneol/Boron Acrylate Polymer. *J. Colloid Interface Sci.* **2022**, *612*, 459–466.

(43) Liu, M.; Li, J.; Li, B. Mannose-Modified Polyethylenimine: A Specific and Effective Antibacterial Agent against *Escherichia Coli*. *Langmuir* **2018**, *34*, 1574–1580.

(44) Liu, G.; Xu, Z.; Dai, X.; Zeng, Y.; Wei, Y.; He, X.; Yan, L.-T.; Tao, L. De Novo Design of Entropy-Driven Polymers Resistant to Bacterial Attachment via Multicomponent Reactions. *J. Am. Chem. Soc.* **2021**, *143*, 17250–17260.

(45) He, T.; Chan, V. Covalent Layer-by-Layer Assembly of Polyethyleneimine Multilayer for Antibacterial Applications. *J. Biomed. Mater. Res., Part A* **2010**, *95A*, 454–464.

(46) Tiller, J. C.; Liao, C.-J.; Lewis, K.; Klivanov, A. M. Designing Surfaces That Kill Bacteria on Contact. *Proc. Natl. Acad. Sci.* **2001**, *98*, 5981–5985.

(47) Ghosh, S.; Das, P.; Ganguly, S.; Remanan, S.; Das, T. K.; Bhattacharyya, S. K.; Baral, J.; Das, A. K.; Laha, T.; Das, N. Ch. 3D-Enhanced, High-Performing, Super-Hydrophobic and Electromagnetic-Interference Shielding Fabrics Based on Silver Paint and Their Use in Antibacterial Applications. *ChemistrySelect* **2019**, *4*, 11748–11754.

(48) Lin, J.; Chen, X.; Chen, C.; Hu, J.; Zhou, C.; Cai, X.; Wang, W.; Zheng, C.; Zhang, P.; Cheng, J.; Guo, Z.; Liu, H. Durably Antibacterial and Bacterially Antiadhesive Cotton Fabrics Coated by Cationic Fluorinated Polymers. *ACS Appl. Mater. Interfaces* **2018**, *10*, 6124–6136.

(49) Zhao, Y.; Guo, Q.; Dai, X.; Wei, X.; Yu, Y.; Chen, X.; Li, C.; Cao, Z.; Zhang, X. A Biomimetic Non-Antibiotic Approach to Eradicate Drug-Resistant Infections. *Adv. Mater.* **2019**, *31*, 1806024.

(50) Chen, C.; Xie, Z.; Zhang, P.; Liu, Y.; Wang, X. Cooperative Enhancement of Fungal Repelling Performance by Surface Photografting of Stereochemical Bi-Molecules. *Colloids Interface Sci. Commun.* **2021**, *40*, 100336.

(51) Sun, X.; Qian, Z.; Luo, L.; Yuan, Q.; Guo, X.; Tao, L.; Wei, Y.; Wang, X. Antibacterial Adhesion of Poly(Methyl Methacrylate) Modified by Borneol Acrylate. *ACS Appl. Mater. Interfaces* **2016**, *8*, 28522–28528.

(52) Wu, J.; Wang, C.; Xiao, Y.; Mu, C.; Lin, W. Fabrication of Water-Resistance and Durable Antimicrobial Adhesion Polyurethane Coating Containing Weakly Amphiphilic Poly(Isobornyl Acrylate) Side Chains. *Prog. Org. Coat.* **2020**, *147*, 105812.

(53) Zhang, D.; Shi, C.; Cong, Z.; Chen, Q.; Bi, Y.; Zhang, J.; Ma, K.; Liu, S.; Gu, J.; Chen, M.; Lu, Z.; Zhang, H.; Xie, J.; Xiao, X.; Liu, L.; Jiang, W.; Shao, N.; Chen, S.; Zhou, M.; Shao, X.; Dai, Y.; Li, M.; Zhang, L.; Liu, R. Microbial Metabolite Inspired β -Peptide Polymers Displaying Potent and Selective Antifungal Activity. *Adv. Sci.* **2022**, *9*, 2104871.

(54) Albuquerque, L. J. C.; Alavarse, A. C.; Carlan da Silva, M. C.; Zilse, M. S.; Barth, M. T.; Belletini, I. C.; Giacomelli, F. C. Sweet Vector for Gene Delivery: The Sugar Decoration of Polyplexes Reduces Cytotoxicity with a Balanced Effect on Gene Expression. *Macromol. Biosci.* **2018**, *18*, 1700299.

(55) Liu, X.; Liu, Y.; Du, J.; Li, X.; Yu, J.; Ding, B. Breathable, Stretchable and Adhesive Nanofibrous Hydrogels as Wound Dressing Materials. *Eng. Regen.* **2021**, *2*, 63–69.

(56) Zhou, J.; Li, M.; Zhong, L.; Zhang, F.; Zhang, G. Aminolysis of Polyethylene Terephthalate Fabric by a Method Involving the Gradual Concentration of Dilute Ethylenediamine. *Colloids Surf., A* **2017**, *513*, 146–152.

(57) Yu, M.; Wang, Z.; Lv, M.; Hao, R.; Zhao, R.; Qi, L.; Liu, S.; Yu, C.; Zhang, B.; Fan, C.; Li, J. Antisuperbug Cotton Fabric with Excellent Laundering Durability. *ACS Appl. Mater. Interfaces* **2016**, *8*, 19866–19871.

(58) Mao, J.; Li, Y.; Wu, T.; Yuan, C.; Zeng, B.; Xu, Y.; Dai, L. A Simple Dual-PH Responsive Prodrug-Based Polymeric Micelles for Drug Delivery. *ACS Appl. Mater. Interfaces* **2016**, *8*, 17109–17117.

(59) Negm, N. A.; Elkholy, Y. M.; Zahran, M. K.; Tawfik, S. M. Corrosion Inhibition Efficiency and Surface Activity of Benzothiazol-3-ium Cationic Schiff Base Derivatives in Hydrochloric Acid. *Corros. Sci.* **2010**, *52*, 3523–3536.